Original Article

# REDUCTION OF TIME AND COST IN PREPARATION OF NANOFIBERS FROM PVA, PEO AND HPMC USING DESIGN-EXPERT® SOFTWARE

## LAYTH J. ABDULREDHA SHAWKA AL-ASADI[1] ID, SARMAD AL-EDRESI[2*] ID

[1]Babil Health Directorate, Babil General Hospital, Babil, Hilla, Iraq. [2]Department of Pharmaceutics and Industrial Pharmacy, Faculty of Pharmacy, University of Kufa, Najaf-52001, Iraq
*Corresponding author: Sarmad Al-Edresi; *Email: s.aledresi@uokufa.edu.iq

## ABSTRACT

**Objective:** The following research aims to formulate nanofibers using a statistical model to reduce time and cost. Nanofibers are nanomaterials composed of a blend of more than one polymer. The selection of the proper exact ratio is challenging, costly and time-consuming.

**Methods:** Nanofibres were prepared from polyvinyl alcohol (PVA), polyethylene oxide (PEO), and hydroxyl propyl methyl cellulose (HPMC) at different concentrations. The experiment used Design-Expert® software (version 13) through full factorial design. A high electrical field was applied to convert the polymeric solution to electrospun nanofibers. Voriconazole, as a triazole drug, was used as a model drug. The entrapment efficiency (EE%) of Voriconazole, fibre diameters and the morphology of nanofibers were analysed using scanning electron microscopy (SEM). The higher desirability of nanofibers was selected.

**Results:** The EE% ranged from 6.7 % to 97.94 %. Fibres diameter ranged from 87.18 to 2500 nm. An SEM analysis revealed long and uniform threads of nanofibers. The solution suggested by the software out of 18 runs resulted in nanofibers having an EE% of 90.3% and a diameter of 87.8 nm±22. 2 SD.

**Conclusion:** Electrospun nanofibres were successfully prepared from 18 runs only. A high loading of model drug was achieved at relatively low numbers of experiments. Time and cost were effectively reduced while maintaining a high desirability for the results.

**Keywords:** Nanotechnology, Electrospinning technique, Nanofibres, Design-Expert® software

## INTRODUCTION

Time, effort, and costs are the main research hindrances in producing and gaining high-quality results [1]. These hindrances are because most experiments are based on many factors and multiple variables. Many attempts were made to deliver high-quality results at a minimum cost [2]. These could be achieved by relying on statistical designs.

Using statistical designs and models in pharmaceutical studies is fundamental to receiving high-accuracy results while reducing the number of runs [3, 4]. Design Expert® software (version 13) provided by Stat-Ease® was used to design the pharmaceutical experiment to develop an empirical model building that improves and optimises process parameters and shows the effect of each variable on the experiment [5]. Design expert® software offers statistical and mathematical analysis of all factors involved in the experiment and its correlation with the desired responses in a three-dimensional manner [6].

Factorial design is one of the Design expert® software models that permits all the independent factors to be changed simultaneously, evaluating each variable effect at every level and displaying the interrelationship among all variables [5, 7]. The statistical method used quantitative data from the related experiment [8].

Nanotechnology is applied to manipulate and prepare compounds or materials in submicron or nanoscale size to produce new structural and physical properties [9, 10]. Nanotechnology is a part of science dealing with materials that have a particle size on a nanometre scale (one billionth of a metre $10^{-9}$) and interfering with characterization, formulation, design, structural modification and application in a wide window of scientific aspects [11, 12]. Nanotechnology plays a vital role in developing new drug delivery systems, which enhance pharmaceutical elements such as drug solubility and permeability, controlling drug release and targeting a specific site of action [13, 14].

Nanofibres are a type of nanosystem that can be produced by various technical methods such as drawing, templet synthesis, freeze-drying, phase separation, self-assembly, and electrospinning [15, 16]. The electrospinning principle involves an electrohydrodynamic technique;

during needle or needleless electrospinning, a solution droplet is electrified to generate a jet, and the jet undergoes stretching and elongation to produce nanofibers [17, 18].

Four major components of the electrospinning device are (a) A high-voltage power supply unit which applies an electrical field between two electrodes, a positively-charged electrode joined with a syringe needle and the negative electrode joined to the collector; (b) A metallic needle from which the charged polymeric solution is pumped to stretch under the high electrical field; (c) A controlled syringe pump and finally; (d) Grounded collectors which collect the resultant fibres [19, 20].

Nanofibres were fabricated using a single or a combination of polymers. A single polymer was not recommended for producing nanofibres because of its lower mechanical properties and higher degradation rates [21]. However, most articles recommend combining polymers to produce homogenous nanofibres with good physical properties [22]. Many polymers were recommended for nanofibre production [23]. However, PVA, PVO and PEO were recommended because PVA has thermal, optical, chemical and electrical stabilities, biosafety, biodegradability, biocompatibility and improved physical and mechanical properties [24, 25]. The PEO is characterised by high adaptability in the electrospinning process, making it easily fabricated to form electrospun nanofibers that are used as a scaffold for various drugs applied in various biomedical aspects [26]. The HPMC polymers have good water solubility but low electrospinability and mechanical properties; therefore, they do not lead to the production of uniform nanofibers. Furthermore, researchers mostly enhance these properties by blending them with natural or synthetic polymers such as PVA, chitosan, PEO, etc. [27, 28].

During the electrospinning process, the solution prepared was pumped from the needle of a syringe called spinneret (which has different inner orifices gauges) at a previously determined flow rate, and the power voltage reached 30 kv. This process produces a pendant droplet due to the surface tension effect of the solution [29].

The following research aimed to reduce the time and cost of producing nanofibres while maintaining high quality and reproducibility.

## MATERIALS AND METHODS

### Materials

Voriconazole pure drug was purchased from Alfyhaa Drug Industries, Basra-Iraq. PVA was purchased from Mese, Germany; PEO was purchased from Micxy reagent, China; HPMC (E5) was purchased from Changsha Goomoo Chemical Technology, China; Absolute Ethanol and deionised water was purchased from Emsure, Germany.

### Methods

#### Preparation of electrospinning solutions

He *et al.* (2020) adapted the method of preparing an electrospinning solution [30]. The solution containing three synthetic biopolymers (PVA, PEO and HPMC) in different concentrations with an active pharmaceutical agent, Voriconazole (as a model drug), was prepared by dissolving each polymer in deionised water separately and stirring overnight using a magnetic stirrer at room temperature. Then, the three polymers (PVA, PEO and HPMC) were in a ratio of 7:2:1, respectively.

Voriconazole was weighed precisely and dissolved in absolute ethanol with gentle stirring for one hour to ensure complete dissolution. It was then added to the mixture of polymeric solution in a ratio of 5% of the total polymers used. Next, the final solution was stirred for 1 hour to become ready to be applied in the electrospinning process. The procedure was adapted from Jia*et al.* (2008) [31].

#### The setting of the electrospinning apparatus

Before starting the electrospinning process, the electrospinning device (Medfusicn MS 2200) was set on several factors to control the whole process. Depending on preliminary studies, the flow rate of solution was set at 1 ml. h$^{-1}$, the separate to collector distance was kept at 15 cm, the temperature of the device chamber was controlled at 20-25 °C, and the relative humidity was adjusted at 30-35, the electrical voltage applied by power supply was reserved at 20 kv, and the ground collector wrapped with aluminium foil and rotate at 600 rpm.

#### Determination of the mixing order of the polymers

Design-Expert®software (version 13) provided by Stat-Ease® company was used to design the pharmaceutical experiment. This software helps to develop an empirical model building that improves and optimises process parameters and shows the effect of each variable on the experiment [8]. It reduces the number of attempts required in the experiments from many tenths attempts to a limited number of attempts within statistical planning that depends on the nature of the variables and the required results. The software set the highest and lowest levels of each parameter participating in the experiment [8]. The PVA was set in the 5-15 g range, PEO in the 1-5 g range, and HPMC in the 0.25-3 g range, depending on previous and preliminary studies. Design-Expert®software detected many centre points in the three-dimensional scope of the experiment. It divided the proposed attempts into several blocks by repeating trials to check the possible hand errors. The design can be augmented as required to increase the probability of factor correlation.

Optimisation of the experiment to reach the desired outcome includes three steps: (a) statistical designing of experiments, (b) estimation of the coefficients through predicting a mathematical model, and (c) guessing the responses and examination of the adequacy of the model within the setup of the experiment [32]. After achieving the statistical analysis (ANOVA) for the proposed attempts with their results, the software offered the optimisation category that enhances the researcher's ability to predict the optimal formulae regarding the highest desirability.

#### Preparation of electrospun nanofibers

The preparation of electrospun nanofibres was adapted from Esentürk İ. *et al.* (2020) [33]. The electrospinning process was applied to solutions prepared previously; the device syringe was filled with the solution and connected to the +ve electrode (cathode), while the –ve electrode (anode) was connected to a rotatable grounded collector, and the process started until the whole solution extruded from the syringe. The nanofibres were rubbed around the foil and collected in a sealed glass container for further examination. Next, fibre diameters and EE% were determined. The compositions of polymeric solutions are listed in table 1.

**Table 1: Composition of formulas proposed by design-expert® software**

| Run | Block | Factor 1 (PVA) (mg) | Factor 2 (PEO) (mg) | Factor 3 (HPMC) (mg) |
|-----|-------|---------------------|---------------------|----------------------|
| 1 | 1 | 15 | 1 | 0.25 |
| 2 | 1 | 5 | 1 | 3 |
| 3 | 1 | 5 | 5 | 0.25 |
| 4 | 1 | 10 | 3 | 1.625 |
| 5 | 1 | 15 | 5 | 3 |
| 6 | 2 | 15 | 1 | 3 |
| 7 | 2 | 5 | 5 | 3 |
| 8 | 2 | 15 | 5 | 0.25 |
| 9 | 2 | 5 | 1 | 0.25 |
| 10 | 2 | 10 | 3 | 1.625 |
| 11 | 3 | 10 | 6.4 | 1.625 |
| 12 | 3 | 10 | 3 | 1.625 |
| 13 | 3 | 18.41 | 3 | 1.625 |
| 14 | 3 | 10 | 0 | 1.625 |
| 15 | 3 | 10 | 3 | 0 |
| 16 | 3 | 10 | 3 | 3.94 |
| 17 | 3 | 10 | 3 | 1.625 |
| 18 | 3 | 1.59 | 3 | 1.625 |

#### Quantification method of voriconazole

Moscoso *et al.* (2020) modified the Voriconazole's quantification method [34, 35]. Voriconazole was solubilised in ethanol with stirring for 15 min, and then UV analysis was conducted.

#### The melting point of voriconazole

Analysis of the melting point of Voriconazole was conducted according to work published by Alkufi and Rashid (2021) [36]. Voriconazole powder was poured into a capillary tube. Then, the capillary loaded with the drug was mounted in the melting point machine (name, model, country). The machine was adjusted to increase the temperature gradually from 25 °C to 150 °C. The powder was visually inspected, and the experiment was terminated when the powder turned into a liquid (melting point temperature). The powder's melting temperature was taken as a melting point.

#### The EE% voriconazole

The EE% was adapted from Aydogdu *et al.* (2019) [37]. The EE% analysis was conducted to determine the ratio of drugs entrapped in the polymers and determined using eq. 1.

$$\text{EE} \ (\%) = \frac{Ve}{Va} \times 100\% \ \ldots\ldots\ldots\ldots \text{Eq. 1}$$

The EE% is the percentage of entrapment efficiency of Voriconazole in the polymers, Ve is Voriconazole measured in nanofiber membranes, and Va symbolises the actual Voriconazole in the electrospinning solution.

### Morphology, size and size distribution of the nanofibres

Morphology analysis was adapted from Aytac *et al.* (2019) [38]. The SEM analysis was conducted to detect electrospun nanofibers' fibre shape and diameter. The electrospun nanofibres from 18 runs were investigated individually by SEM (FEI, quanta 450, Czech). Images revealed the morphology of resultant nanofibers and measured their diameters in nanometres. The average number of records was calculated using a standard deviation estimation. The setting of the SEM machine was conducted on voltage 25.00 kv, magnification 23624 and width (8.3-9.3 mm).

### Purity and conjugation of voriconazole

The purity and possible conjugation of voriconazole to the matrix of the polymeric nanofibres were tested using FTIR [39]. The analysis method was adapted from Sinha *et al.* (2013) with minor modifications [40].

### Determination of the optimised formula

Depending on statistical analysis achieved by Design-Expert® software, the optimised formula (or formulas) would be obtained depending on the analysis of data and the highest desirability for each factor and response. Therefore, the software introduced many solutions (optimum formulas) regarding the highest value of EE% and lowest value of nanofiber diameter. The chosen formula must have the highest desirability based on statistical analysis. Nanofibers obtained from the optimised formula will be investigated further and compared with the suggested theoretical solution [41].

### Statistical analysis of suggested formulas

The Design-Expert® software was used to determine several statistical concepts such as the desirability of factors relationship, Pareto charts, Half standard plots, box Cox plots for power transform, three-dimensional surface plot, the interaction of each factor with each response, ANOVA tests and mathematical equations of each response and histograms [42].

### RESULTS AND DISCUSSION

### Quantification of voriconazole

The λ max of Voriconazole was absorbed at 256 nm. This result corresponded to the result of voriconazole λ max measured by Rui Chen and his co-workers (2020), who noted that Voriconazole was absorbed in wavelength 256 nm using a UV visible spectrophotometer [43]. According to Beer's law, the calibration curve was constructed as a linear line giving regression coefficient

($R^2$= 0.9983). The line equation was generated, yielding the intercept and the slope as shown in Equation 2.

$$Y = 0.0186\ X \dots\dots\ Eq.\ 2$$

Where Y was absorbency in nm, and X was a concentration in μg/ml. These results corresponded to the voriconazole finding reported by Mori *et al.*, 2017 [44].

### The melting point of voriconazole

The melting point of voriconazole pure drug measured by the capillary tube method was found to be 131 °C which agreed with the published articles by Szepiński, E. *et al.* 2017 and Supraja K. *et al.* 2020 indicated that the purity of Voriconazole was high.

### Preparation of electrospun nanofibers

The electrospinning process was achieved on the 18 runs listed in table 2, and resultant fibres were removed from the foils and collected in a sealed container. The electrospun nanofibres were investigated to determine the shape and diameter of fibres and the EE% of Voriconazole in the polymers. The results of all responses are illustrated in fig. 1 and listed in table 2.
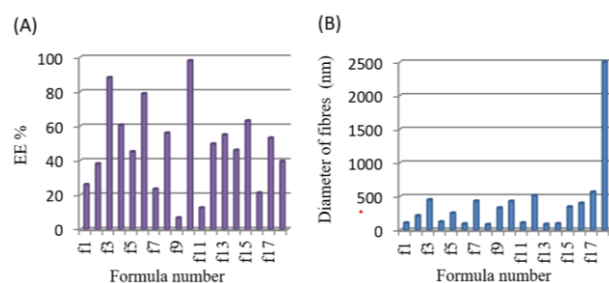


**Fig. 1: Results of nanofibres investigations. (A) The EE% of voriconazole in the polymers; and (B) The nanofiber's diameter in nm. Data is given in mean±SD, n=3**

The Design-Expert®software statistically analysed the results of all factors and responses and the correlation among them in three-dimensional levels. Therefore, the study includes the effect of each factor (polymer) on entrapment efficiency. The correlation between factors and the EE% is determined in Equation 3.

$$EE\ (\%) = -124.41 + 13.6601 \times A + 61.3734 \times B + 79.8603 \times C + -4.92648 \times AB + -6.10118 \times AC + -32.1586 \times BC + 2.48991 \times ABC \dots\dots\dots\dots\ Eq.\ 3$$

Where EE% was the entrapment efficiency, A was PVA, B was PEO, and C was HPMC.

**Table 2: Responses of electrospinning processes, EE% and fibre diameter**

| Run no. | Block | Response 1 EE% (%) | Response 2 fibre diameter (nm)* |
|---|---|---|---|
| 1 | 1 | 25.98 | 106.6±24.73 |
| 2 | 1 | 38.07 | 214.0±59.11 |
| 3 | 1 | 88.11 | 450.9±77.13 |
| 4 | 1 | 37.58 | 122.6±8.890 |
| 5 | 1 | 45.1 | 252.5±43.16 |
| 6 | 2 | 78.76 | 92.6±29.150 |
| 7 | 2 | 23.4 | 430.4±35.20 |
| 8 | 2 | 55.95 | 82.9±22.434 |
| 9 | 2 | 6.7 | 330.2±103.3 |
| 10 | 2 | 61.94 | 428.2±170.3 |
| 11 | 3 | 12.5 | 106.8±39.55 |
| 12 | 3 | 49.61 | 514.0±259.7 |
| 13 | 3 | 54.91 | 87.2±25.691 |
| 14 | 3 | 46 | 94.9±13.116 |
| 15 | 3 | 63.05 | 344.3±269.4 |
| 16 | 3 | 21.22 | 399.7±44.94 |
| 17 | 3 | 47.05 | 565.7±197.6 |
| 18 | 3 | 39.5 | 2000±234.25 |

*Data is given in mean±SD, n=3.

Fit statistics provided by Design-Expert® software implied that the calculated standard deviation was 17.88, the mean was 46.19, the correlation of variance was C. V. % = 38.72, regression $R^2$= 0.7584, and adequate precision was 5.6828. Adequate precision measures the signal-to-noise ratio. When the ratio was more significant than 4, it was considered desirable. Therefore, the ratio obtained by Design-Expert®software (5.683) indicates an adequate signal with good desirability. The p-value of (ABC) was found to be 0.0456, less than 0.05, indicating that the model has a significant correlation and that the three polymers significantly affect entrapment efficiency.

The polymers used in the electrospinning process have variable effects on voriconazole EE% in polymer mixtures. The half-normal plot and Pareto chart showed that both PVA and PEO positively affect entrapment efficiency; thus, when their concentration increased, the EE% increased. The effect of PVA on EE% is superior to that of PEO. The HPMC has a negative impact on entrapment efficiency, meaning high concentration leads to a decrease in entrapment efficiency.

Results of the SEM analysis are listed in table 2, with a wide range of fibre diameters starting from 87.2 nm (run 13) to 2500 nm (run 18). Run 18 did not produce true nanofibers due to the deficient concentration of PVA. The statistical analysis revealed that the effect of each polymer (factor) on the diameter size of the electrospun

nanofiber was vast. Therefore, there is a correlation between factors A, B and C and fibre diameter as expressed in equation 5.

Fiber dimeter = 374.055+-3.19245 × A+214.052 × B+268.017 × C+-21.8677 × AB+-30.421 × AC+-106.428 × BC+11.9123 × ABC .... Eq. 5

Where A is PVA, B is PEO, and C is HPMC.

The provided fit statistic implied that the calculated standard deviation was 588.46, the mean was 395.75, the correlation of variance was C. V. % = 141.11, and regression $R^2$= 0.3169. The p-value of (ABC) is 0.0496, less than 0.05, indicating a significant model. The three polymers used in the electrospinning process have a movable effect on electrospun fibre diameter. The PVA have a negative impact on fibre diameter. Therefore, when their concentration increased, the fibre decreased.

On the other hand, the PEO and HPMC positively affect fibre diameter, leading to an increment in diameter. Therefore, increasing the concentration of PEO and HPMC would increase the fibre's diameter. However, the effect's superiority was to PEO compared with HPMC, which appears in the Pareto chart indicating the little impact of a factor on fibre diameter. The most superior negative effect on fibre diameter was correlated with the increment of factor PVA. The half-normal plot and Pareto chart are reported in fig. 2.
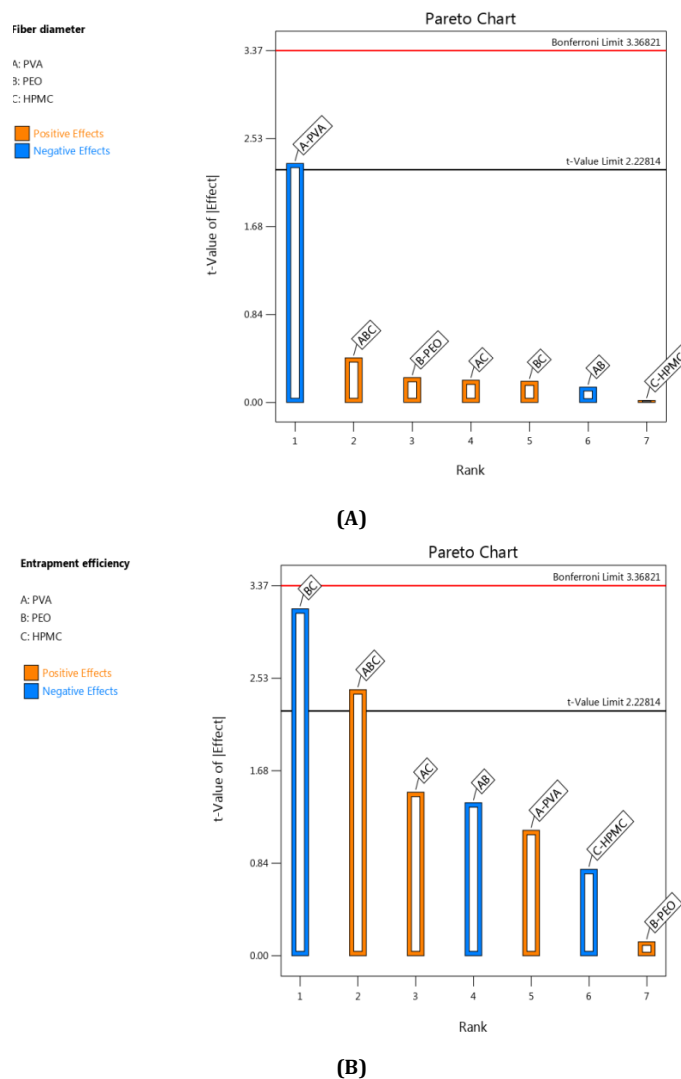


**(A)**



**(B)**

**Fig. 2: Pareto chart of the variables. (A) The effect of polymers on fibre diameters; (B) The effect of polymers on entrapment efficiency**

Several factors affect electrospinning and play an essential role in forming electrospun nanofibers' shape, length, entanglement and

diameter size. The properties of each polymer used in solution preparation and the properties of the final solution would affect the

morphology of fibres. The PVA concentration directly affects the diameter of the resulting fibres. Increasing PVA concentration would lead to the formation of uniform fibres without beads and decreasing diameter. Also, increasing PVA concentration increases the viscosity of the solution, hence keeping the get flying and preventing it from breaking into tiny drops. Therefore, the concentration of PVA must be at a higher level (upper limit). Caution must be taken not to exceed the upper limits as this might produce smooth fibres with diameter. Jia and his colleagues (2008) highlighted that adding a low concentration of PEO to PVA decreases the surface tension of the solution and is subsequently overcome by the applied electrical field, increasing the spinnability of the solution.
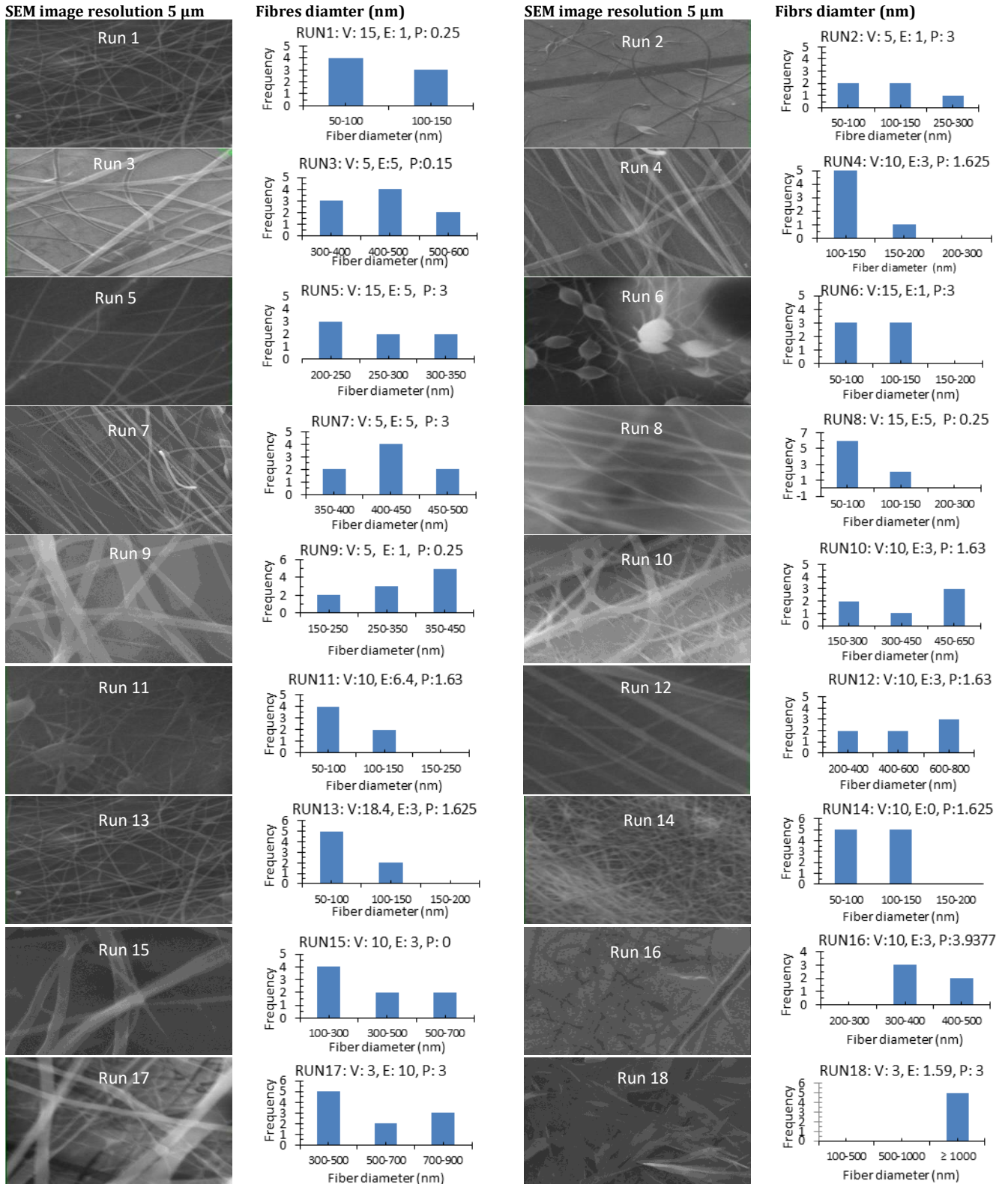


Fig. 3: Nanofibres SEM images with nanofiber diameter frequencies. The PVA, PEO and HPMC were symbolised as V, E and P. Data are given in mean±SD, n=3

The HPMC have poor electrospinnability propriety, hindering the formation of uniform and smooth nanofibers. Adding PEO polymers in low concentration to the HPMC solution would improve the electrospinnability of the solution. Also, the viscosity would be modified to ensure an intact jet during the process [31]. However, adding PEO would generate repulsive forces among molecules, increasing the fibres' entanglement and ultimately improving nanofibre formation. These results agreed with Aydogdu, A. *et al.* (2018) and Grip, J. *et al.*(2020) [45, 46]. Increasing the concentration of PEO and HPMC would increase the fibre's diameter and distribution due to the higher viscosity of the solution. High viscosity would affect the stretching of the solution, resulting in reduced jet path and formation of fibres with large diameters as found in runs 3, 5 and 7, and these results were consistent with the finding of Aydogdu, A. *et al.* (2018) [45]. The diameter of the fibres could be reduced when the conductivity of the solution increased. Therefore, the recommendation was to use a high-conductivity solution or add salts [30].

The morphology of nanofibers would be affected by device parameters such as flow rate, voltage and distance from the collector. Also, nanofibres' properties could be changed due to temperature and humidity. The bead formation appears with a low concentration of PVA (run 2) or a high concentration of PEO and HPMC (runs 6 and 11), as shown in fig. 3. Therefore, increasing PVA concentration leads to beads' disappearance and smooth fibres'

formation. Nageeb El-Helaly (2021) and Silva J. A. *et al.* (2021) reported similar results [47, 48]. Kalluri*et al.*(2021)[49] studied the relationship between the fibre diameter, bead diameter and flow rate. Thus, they concluded that better fibre uniformity and bead formation were needed at a high flow rate. These results appear clearly in run two and run six and agree with Silva *et al.*(2021) results [50], who reported that only the concentration of PVA (≥ 15%) could produce uniform nanofibers when using the lower molecular weight of PVA (67,000). Fibre diameter of 15% PVA and more appeared to be in the range 87.11 to 252.5 nm with uniform fibres and disappearance of beads except in run 6, where the beads appear due to increasing the concentration of HPMC as highlighted by Grip*et al.* (2018) [46].

**Determination of the optimised formula**

The obtained data were analysed statistically *via the* Design-Expert® software, which suggested several formulae with various concentrations of each polymer varied in their desirability to reach the optimum target. Thirty solutions were proposed to achieve the optimal formula from high to low desirably, as listed in table 2, offering high EE% and low fibre diameter. The selected formula was formula 1 (table 3), which has the highest desirability, 95.2%, and offered better responses, with 89.85 % of EE% and 94.13 nm of nanofibres diameter.
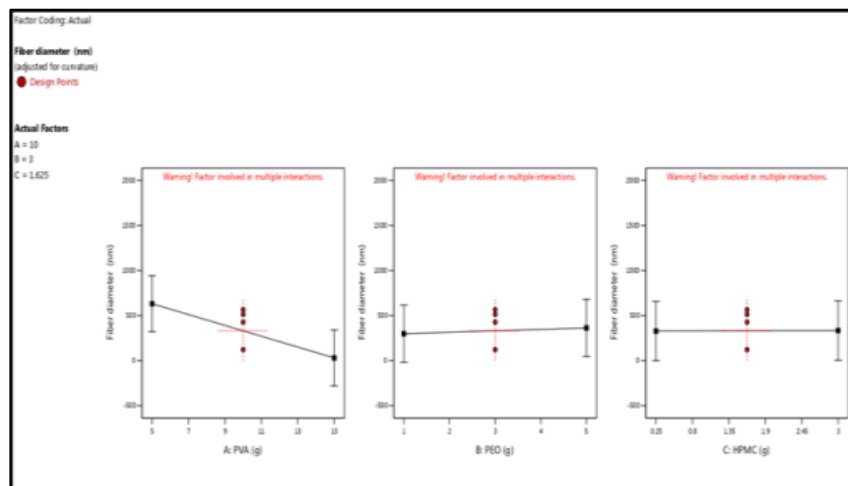


**(A)**
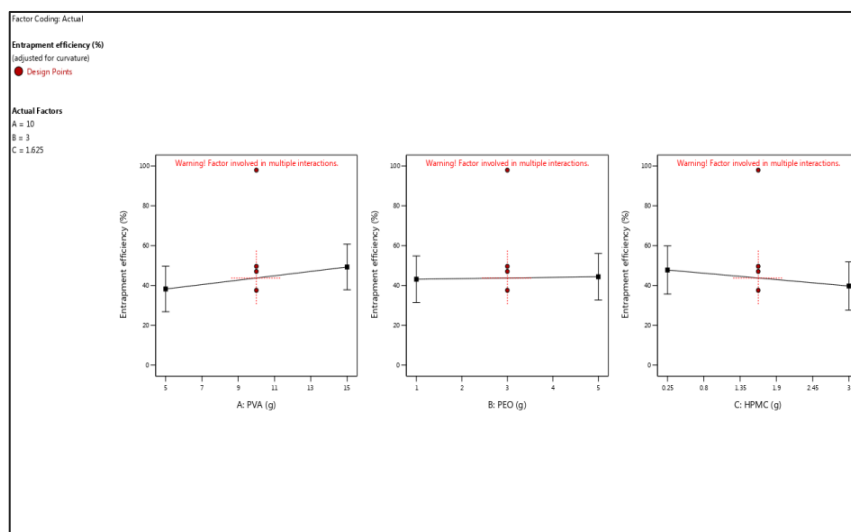


**(B)**

**Fig. 4: Effect of the polymers on nanofibre formation. (A)The effect of polymers on entrapment efficiency; (B) The effect of polymers on fibre diameters**

**Table 3: Suggested values of the independent variable for optimal formula preparation provided by design-expert® software**

| S. No. | Number | PEO | HPMC | Fibres diameter | EE% | Desirability | Best formula |
|---|---|---|---|---|---|---|---|
| 1 | 18.000 | 1.000 | 0.250 | 94.130 | 89.844 | 0.952 | Selected |
| 2 | 18.000 | 1.000 | 0.264 | 91.732 | 89.600 | 0.951 | |
| 3 | 18.000 | 1.028 | 0.250 | 89.918 | 89.178 | 0.949 | |
| 4 | 18.000 | 1.000 | 0.301 | 85.430 | 88.964 | 0.949 | |
| 5 | 18.000 | 1.000 | 0.313 | 83.268 | 88.749 | 0.948 | |
| 6 | 17.901 | 1.000 | 0.250 | 97.061 | 89.069 | 0.947 | |
| 7 | 18.000 | 1.007 | 0.326 | 80.135 | 88.376 | 0.946 | |
| 8 | 18.000 | 1.131 | 0.250 | 74.133 | 86.680 | 0.936 | |
| 9 | 17.819 | 1.112 | 0.250 | 82.782 | 85.803 | 0.931 | |
| 10 | 18.000 | 1.107 | 0.463 | 43.755 | 83.865 | 0.920 | |
| 11 | 18.000 | 6.000 | 3.000 | 344.383 | 95.645 | 0.918 | |
| 12 | 18.000 | 5.999 | 2.989 | 340.144 | 95.120 | 0.916 | |
| 13 | 17.955 | 5.993 | 3.000 | 343.875 | 95.095 | 0.915 | |
| 14 | 18.000 | 5.828 | 3.000 | 319.624 | 93.815 | 0.915 | |
| 15 | 18.000 | 6.000 | 2.967 | 332.368 | 94.144 | 0.913 | |
| 16 | 17.250 | 1.000 | 0.250 | 116.384 | 83.966 | 0.912 | |
| 17 | 18.000 | 6.000 | 2.957 | 328.638 | 93.679 | 0.912 | |
| 18 | 18.000 | 6.000 | 2.923 | 315.882 | 92.086 | 0.907 | |
| 19 | 17.760 | 6.000 | 2.996 | 345.795 | 92.944 | 0.903 | |
| 20 | 17.552 | 5.972 | 3.000 | 345.589 | 90.629 | 0.891 | |
| 21 | 16.847 | 1.000 | 0.250 | 128.361 | 80.812 | 0.891 | |
| 22 | 18.000 | 4.738 | 3.000 | 162.108 | 82.170 | 0.891 | |
| 23 | 17.832 | 5.035 | 3.000 | 209.158 | 83.971 | 0.889 | |
| 24 | 8.592 | 6.000 | 0.250 | 499.149 | 97.940 | 0.885 | |
| 25 | 8.576 | 5.987 | 0.250 | 500.751 | 97.940 | 0.884 | |
| 26 | 8.625 | 6.000 | 0.250 | 495.034 | 97.485 | 0.884 | |
| 27 | 8.534 | 6.000 | 0.271 | 505.897 | 97.939 | 0.883 | |
| 28 | 8.471 | 6.000 | 0.250 | 514.150 | 99.594 | 0.880 | |
| 29 | 8.417 | 5.872 | 0.256 | 517.072 | 97.940 | 0.880 | |
| 30 | 17.685 | 4.925 | 3.000 | 197.394 | 81.686 | 0.879 | |

The proposed optimal formula tends to increase the concentration of factor A (PVA) to the highest level of 18g.100 ml$^{-1}$ due to the statistical results that PVA has a positive effect on EE% and a negative effect on fibre diameter. Therefore, increasing the concentration would improve EE% and reduce fibre diameter, as shown in fig. 5. Nageeb El-Helaly (2021) reported that PEO and HPMC have poor electrospinable properties and could be improved by increasing the concentration of PVA [48]. However, factor B (PEO) have a negative effect on EE% and a positive impact on fibre diameter. Therefore, the selected solution had the lowest level of PEO 1g.100 ml$^{-1}$, consistent with the result reported by Tam and his colleagues (2017) [51], who studied the effect of HPMC concentration on the electrospinnability of polymeric solution. They found that adding HPMC in a concentration exceeding 2.86% would eliminate electrospinning owing to the high viscosity. The preliminary studies carried out in this experiment have found similar results, enforced using a blend of polymers, including PEO [51].

Adding HPMC polymer to the solution stabilises the fibre network; however, mixing Voriconazole with HPMC only forms homogeneous nanofibers. Therefore, PEO and PVA polymers were added to increase the electrospinnability of the solution and produce uniform and stable nanofibers with low diameters. Tam *et al.* (2017) and Nageeb El-Helaly (2021) have established similar results [48, 51]. Factor C (HPMC) has a negative effect on EE% and a positive effect on fibre diameter. Therefore, the concentration of HPMC reduced to the lowest value, 0.25 g.100 ml$^{-1}$, as shown in fig. 5 and 6.

Further nanofibres were prepared and evaluated depending on the proposed optimal formula to compare practical and predicted values, as clarified in table 3.2. The practical calculated EE% was 90.3%, while the predicted one was 89.8%. This result indicates high agreement between the sensible and predicted values with an accuracy of 99.5 %. Thus, it ensured that the procedure was highly robust and accurate [4].
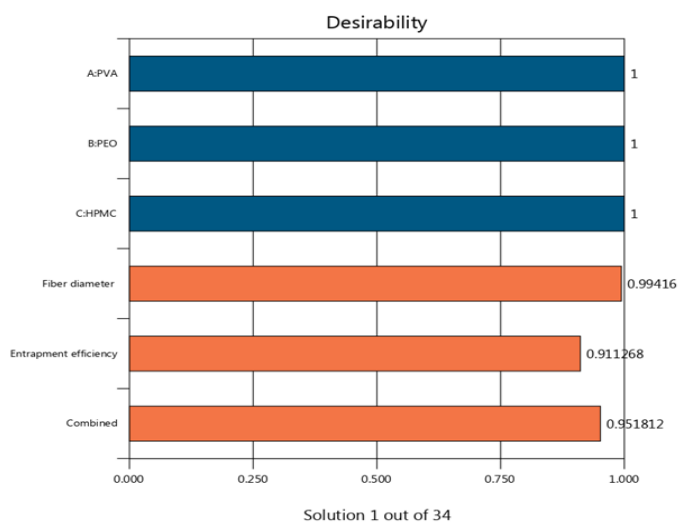


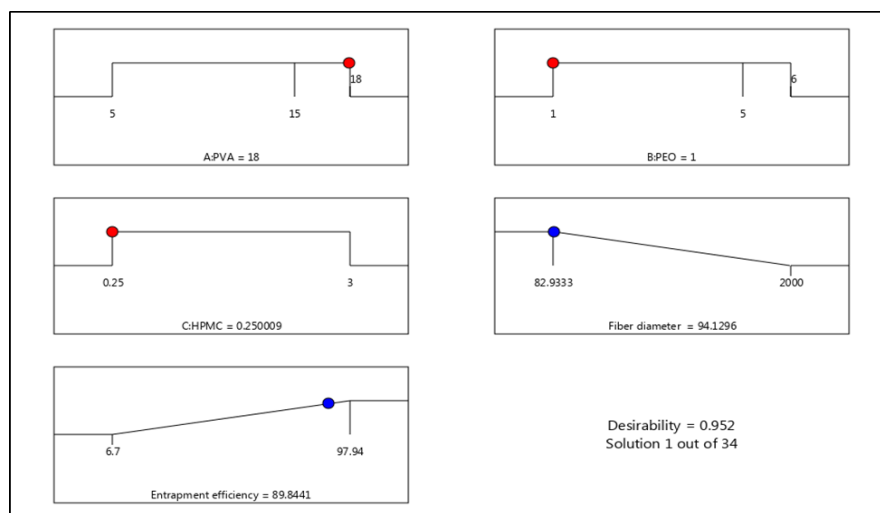**Fig. 5: The desirability of the predicted optimum formula**

**Fig. 6: Effect of different variables on the desirability**

**Fourier transform infrared FTIR studies**

The pure voriconazole spectrum showed the presence of hydroxyl group (O-H) stretching at 3188.82 cm⁻¹, Carbon Nitrogen (C-N) aryl stretching at 1504.94-1450.04 cm⁻¹ and C-F stretching at 1408.16-1127.38 cm⁻¹, C-H alkane stretching at 3045.69-2880,97 cm⁻¹, C=C aromatic bond appeared at 2000-1618.28 cm⁻¹ and finally $CH_3$ at 1377.53 cm⁻¹as shown in fig. 7.
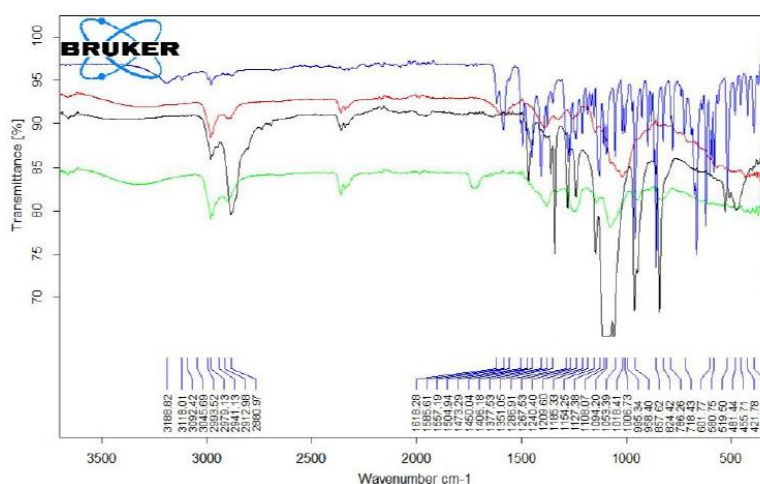


**Fig. 7: FTIR spectrum of voriconazole pure drug and three polymers. Blue: voriconazole, red: PVA, black, PEO and green: HPMC**

The PVA absorption bonds appeared at 3289.4 cm⁻¹ for the hydroxyl group (O–H), while C⬚H bonds were at 2973.22-2935.7 cm⁻¹, and CO was at 1084 cm⁻¹, as shown in fig. 7. The PEO polymer has a characterised absorption bonds (C–H) stretching of the $CH_2$ group appeared at 2881.72 cm⁻¹ for $CH_2$ wagging bonds, 1279.02 and 1240.63 cm⁻¹ and 960.773 $CH_2$ for twisting bonds, and 1466.34 cm⁻¹, which related to gauche $CH_2$ scissor motion, while 1486 cm⁻¹ assigned to the trans-$CH_2$ scissor motion [52].

Other peaks are related to (C–O–C) stretching at 1059.47 cm⁻¹ and 1096.13 cm⁻¹, as illustrated in fig. 7. The HPMC polymer exhibited the absorption bands at 1117.01 cm⁻¹, 2980.45 cm⁻¹ and 3350 cm⁻¹, which recognised the stretching vibration C-O, C-H, and O-H groups, respectively, indicating the stretching vibration of each. Also, the $CH_3$ band appears at 1396.37 cm⁻¹, and the $CH_2$ band is at 1462 cm⁻¹ [53]. The suppository base PEG demonstrated the absorption bands at 2833.46 cm⁻¹ for C-H stretching at 1466.11 cm⁻¹and 955.25 cm⁻¹ for $CH_2$ twisting at 1359.11 cm⁻¹ for $CH_3$at1359.11 cm⁻¹and 1101.64 cm⁻¹ for C-O [54]. All the spectral FTIR charts of all components of the dosage form are illustrated in fig. 7.

Adding PEO polymer to HPMC polymer led to an increase in the intensity of $CH_2$ stretching at 2884.5 cm⁻¹. The PEO crystallinity was depressed when blended with HPMC polymer, and the shape, wavelength and intensity of the C-O-C stretching, which related to the interaction of PEO and HPMC, which shifted the absorbency to 1127.38 cm⁻¹in comparison with pure PEO at 1096.13 cm⁻¹. The prominent characteristic peaks of Voriconazole were not changed in the FTIR spectrum of the final formula, suggesting that Voriconazole was incorporated within the nanofibers [33].

**CONCLUSION**

Preparation of nanofibres loaded with a model drug, Voriconazole, was successfully achieved from a blend of PVA/PEO/HPMC polymers using an electrospinning technique. What makes these nanofibres different is that they were prepared with the aid of Design–Expert® software. Polymer effects on structure, diameter, morphology and EE% were studied and investigated relatively quickly and with low effort and cost. Conjugations between statistical software and practical experiments have significantly decreased time and reduced cost by using fewer materials than the conventional try-and-error method.

**FUNDING**

Nil

## AUTHORS CONTRIBUTIONS

All authors have contributed equally

## CONFLICT OF INTERESTS

Declared none

## REFERENCES

1. Salal AY, Abbas HK, Abdul Razzaq IF. Quality control and testing evaluation of various metoprolol tartrate (50 mg) tablets available in iraq market. J Med Chem Sci. 2023;6(3):606-12. doi: 10.26655/jmchemsci.2023.3.17.

2. Behera SK, Meena H, Chakraborty S, Meikap BC. Application of response surface methodology (RSM) for optimization of leaching parameters for ash reduction from low-grade coal. Int J Min Sci Technol. 2018;28(4):621-9. doi: 10.1016/j.ijmst.2018.04.014.

3. Aledresi SS, Alshaibani AJ, Abood AN. Enhancing the loading capacity of kojic acid dipalmitate in liposomes. Lat Am J Pharm. 2020;39(7):1-7.

4. Al-Hamadani MH, Al-Edresi S. Formulation and characterization of hydrogel of proniosomes loaded diclofenac sodium. Int J Drug Deliv Technol. 2022;12(1):132-6. doi: 10.25258/ijddt.12.1.24.

5. Korycka P, Mirek A, Kramek Romanowska K, Grzeczkowicz M, lewińska D. Effect of electrospinning process variables on the size of polymer fibers and bead-on-string structures established with a 23 factorial design. Beilstein J Nanotechnol. 2018;9(1):2466-78. doi: 10.3762/bjnano.9.231, PMID 30345211.

6. Verma D, Thakur PS, Padhi S, Khuroo T, Talegaonkar S, Iqbal Z. Design expert assisted nanoformulation design for co-delivery of topotecan and thymoquinone: optimization, *in vitro* characterization and stability assessment. J Mol Liq. 2017;242:382-94. doi: 10.1016/j.molliq.2017.07.002.

7. Abdulrazzaq IF, Salal YA, Abdul Hasan MT, Abbas HK, Hasan Al-Gburi KM. A comparative study of quality control testing of mefenamic acid tablets in Iraq. Int J App Pharm. 2022;14(6):127-30. doi: 10.22159/ijap.2022v14i6.46251.

8. Chan S, Jankovic J, Susac D, Saha MS, Tam M, Yang H. Electrospun carbon nanofiber catalyst layers for polymer electrolyte membrane fuel cells: structure and performance. J Power Sources. 2018;392:239-50. doi: 10.1016/j.jpowsour.2018.02.001.

9. Aledresi SS, Abdulrazza IF, Alshaibani AJ. Enhancing the solubility of nimesulide by loading to a nanoemulsion. Lat Am J Pharm. 2020;39(11):2299-308.

10. Giongo JL, Vaucher RD, Ourique AF, Steffler MC, Frizzo CP, Hennemman B. Development of nanoemulsion containing pelargonium graveolens oil: characterization and stability study. Int J Pharm Pharm Sci. 2016;8(12):271-6. doi: 10.22159/ijpps.2016v8i12.15108.

11. Bayda S, Adeel M, Tuccinardi T, Cordani M, Rizzolio F. The history of nanoscience and nanotechnology: from chemical-physical applications to nanomedicine. Molecules. 2019;25(1):1-15. doi: 10.3390/molecules25010112, PMID 31892180, PMCID PMC6982820.

12. Wannas AN, Abdul Hasan MT, Mohammed Jawad KK, Razzaq IF. Preparation and *in vitro* evaluation of Self-Nano emulsifying drug delivery systems of ketoprofen. Int J App Pharm. 2023;15(3):71-9. doi: 10.22159/ijap.2023v15i3.46892.

13. Wen MM, Farid RM, Kassem AA. Nano-proniosomes enhancing the transdermal delivery of mefenamic acid. J Liposome Res. 2014;24(4):280-9. doi: 10.3109/08982104.2014.911313, PMID 24779560.

14. Sarvan VH, Vashisth H. Types and application of pharmaceutical nanotechnology: a review. Int J Curr Pharm Sci. 2023;15(3):14-8. doi: 10.22159/ijcpr.2023v15i3.3010.

15. Flayeh AA, Kadhim HJ. Effect of natural dye on the properties of electrospun multiwall carbon nanotubes/polystyrene nanocomposites nanofibers. J Vis Exp. 2021;9(3):1154-64.

16. Keshvardoostchokami M, Majidi SS, Huo P, Ramachandran R, Chen M, liu B. Electrospun nanofibers of natural and synthetic polymers as artificial extracellular matrix for tissue engineering. Nanomaterials (Basel). 2020;11(1):1-23. doi: 10.3390/nano11010021, PMID 33374248.

17. Xue J, Wu T, Dai Y, Xia Y. Electrospinning and electrospun nanofibers: methods, materials, and applications. Chem Rev. 2019;119(8):5298-415. doi: 10.1021/acs.chemrev.8b00593, PMID 30916938.

18. Madapally VD, MP. Fabrication of nanofibres by electrospinning using keratin from waste chicken feathers, pva and agnps. Int J Pharm Pharm Sci. 2019;11(8):78-84. doi: 10.22159/ijpps.2019v11i8.33637.

19. Wang C, Wang J, Zeng L, Qiao Z, Liu X, Liu H. Fabrication of electrospun polymer nanofibers with diverse morphologies. Molecules. 2019;24(5):1-33. doi: 10.3390/molecules24050834, PMID 30813599.

20. Augustine R, Rehman SR, Ahmed R, Zahid AA, Sharifi M, Falahati M. Electrospun chitosan membranes containing bioactive and therapeutic agents for enhanced wound healing. Int J Biol Macromol. 2020;156:153-70. doi: 10.1016/j.ijbiomac.2020.03.207, PMID 32229203.

21. Adeli H, Khorasani MT, Parvazinia M. Wound dressing based on electrospun PVA/chitosan/starch nanofibrous mats: fabrication, antibacterial and cytocompatibility evaluation and *in vitro* healing assay. Int J Biol Macromol. 2019;122:238-54. doi: 10.1016/j.ijbiomac.2018.10.115, PMID 30342125.

22. Wilk S, Benko A. Advances in fabricating the electrospun biopolymer-based biomaterials. J Funct Biomater. 2021;12(2):1-32. doi: 10.3390/jfb12020026, PMID 33923664.

23. Lekshmi NC, SV, Kumari RS, Bharath MS, SJ, JR. Synthesis of nanofibre and silver nanoparticles from coelomic fluid of earthworm, eudrilus eugeniae and pontoscolex corethrurus and its antimicrobial potency. Asian J Pharm Clin Res. 2014;7(1):177-82.

24. Zhang Z, Kong l, Lv M, Yao Y, Gao l, Zhou R, Ma W, li J. PVA enema ameliorates DSS-induced acute colitis in mice. BMC Gastroenterology. 2023;23(1):1-12. doi: 10.1186/s12876-023-03005-w, PMID: 37904100.

25. Huang R, Tao Z, Wu L, Shen J, Xu W. Investigation of workability and mechanical properties of PVA fiber-reinforced phosphogypsum-based composite materials. Materials (Basel, Switzerland). 2023;16(12):1-19. doi: 10.3390/ma16124244, PMID 37374428, PMCID PMC10300962.

26. Kyzioł A, Michna J, Moreno I, Gamez E, Irusta S. Preparation and characterization of electrospun alginate nanofibers loaded with ciprofloxacin hydrochloride. Eur Polym J. 2017;96:350-60. doi: 10.1016/j.eurpolymj.2017.09.020.

27. Aydogdu A, Yildiz E, Ayhan Z, Aydogdu Y, Sumnu G, Sahin S. Nanostructured poly(lactic acid)/soy protein/HPMC films by electrospinning for potential applications in food industry. Eur Polym J. 2019;112:477-86. doi: 10.1016/j.eurpolymj.2019.01.006.

28. Balogh A, Farkas B, Verreck G, Mensch J, Borbas E, Nagy B. AC and DC electrospinning of hydroxypropylmethylcellulose with polyethylene oxides as a secondary polymer for improved drug dissolution. Int J Pharm. 2016;505(1-2):159-66. doi: 10.1016/j.ijpharm.2016.03.024, PMID 26997426.

29. Yu DG, Li JJ, Williams GR, Zhao M. Electrospun amorphous solid dispersions of poorly water-soluble drugs: a review. J Control Release. 2018;292:91-110. doi: 10.1016/j.jconrel.2018.08.016, PMID 30118788.

30. He M, Chen M, Dou Y, Ding J, Yue H, Yin G. Electrospun silver nanoparticles-embedded feather keratin/poly(vinyl alcohol)/poly(ethylene oxide) antibacterial composite nanofibers. Polymers. 2020;12(2):1-14. doi: 10.3390/polym12020305.

31. Jia Z, Li Q, liu J, Yang Y, Wang L, Guan Z. Preparation and properties of poly (vinyl alcohol) nanofibers by electrospinning. J Polym Eng. 2008;28(1-2):87-100. doi: 10.1515/POLYENG.2008.28.1-2.87.

32. Choi SY, Kim SH. Knowledge acquisition and representation for high-performance building design: a review for defining requirements for developing a Design Expert system. Sustainability. 2021;13(9):1-36. doi: 10.3390/su13094640.

33. Esenturk I, Balkan T, Ozhan G, Dosler S, Gungor S, Erdal MS. Voriconazole incorporated nanofiber formulations for topical application: preparation, characterization and antifungal activity studies against *Candida* species. Pharm Dev Technol. 2020;25(4):440-53. doi: 10.1080/10837450.2019.1706563, PMID 31851857.

34. Moscoso R, Alvarez Lueje A, Squella JA. Nanostructured interfaces containing MWCNT and nitro aromatics: a new tool to determine nimesulide. Microchem J. 2020;159:1-6. doi: 10.1016/j.microc.2020.105361.

35. Abdul Hasan MT, Al-Shaibani AJ, Wannas AN, Hasan Al-Gburi KM. Quality control testing of conventional clopidogrel bisulfate tablets marketed in Iraq. Int J App Pharm. 2022;14:221-5. doi: 10.22159/ijap.2022v14i1.43331.

36. Alkufi HK, Rashid AM. Enhancement of the solubility of famotidine solid dispersion using natural polymer by solvent evaporation. Int J App Pharm. 2021;13(3):193-8. doi: 10.22159/ijap.2021v13i3.40934.

37. Aydogdu A, Sumnu G, Sahin S. Fabrication of gallic acid loaded hydroxypropyl methylcellulose nanofibers by electrospinning technique as active packaging material. Carbohydr Polym. 2019;208:241-50. doi: 10.1016/j.carbpol.2018.12.065, PMID 30658797.

38. Aytac Z, Ipek S, Erol I, Durgun E, Uyar T. Fast-dissolving electrospun gelatin nanofibers encapsulating ciprofloxacin/cyclodextrin inclusion complex. Colloids Surf B Biointerfaces. 2019;178:129-36. doi: 10.1016/j.colsurfb.2019.02.059, PMID 30852264.

39. Abd El Gawad S, Marzouk M, Ammar A. Preparation and evaluation of sustained release matrix formulations of voriconazole. Al-Azhar Journal of Pharmaceutical Sciences. 2023;67(1):19-36. doi: 10.21608/ajps.2023.311244.

40. Sinha B, Mukherjee B, Pattnaik G. Poly-lactide-co-glycolide nanoparticles containing voriconazole for pulmonary delivery: *in vitro* and *in vivo* study. Nanomedicine. 2013;9(1):94-104. doi: 10.1016/j.nano.2012.04.005, PMID 22633899.

41. Hussein S, Abd-Elnaiem A, Ali N, Mebed A. Enhanced thermo-mechanical properties of poly(vinyl alcohol)/Poly(vinyl pyrrolidone) polymer blended with nanographene. Curr Nanosci. 2021;16(6):994-1001. doi: 10.2174/1573413716666200310121947.

42. Mohamed DF, Mahmoud OA, Mohamed FA. Preparation and evaluation of ketotifen suppositories. Journal of Advanced Biomedical and Pharmaceutical Sciences. 2020;3(1):10-22. doi: 10.21608/jabps.2019.19318.1059.

43. Chen R, Zhang T, Bao S, liu Y, Xu X. Formulation and characterization of voriconazole nanospray dried powders. Pharm Dev Technol. 2020;25(7):815-22. doi: 10.1080/10837450.2020.1741618, PMID 32178565.

44. Mori NM, Patel P, Sheth NR, Rathod lV, Ashara KC. Fabrication and characterization of film-forming voriconazole transdermal spray for the treatment of fungal infection. Bull Fac Pharm Cairo Univ. 2017;55(1):41-51. doi: 10.1016/j.bfopcu.2017.01.001.

45. Aydogdu A, Sumnu G, Sahin S. A novel electrospun hydroxypropyl methylcellulose/polyethylene oxide blend nanofibers: morphology and physicochemical properties. Carbohydr Polym. 2018;181:234-46. doi: 10.1016/j.carbpol.2017.10.071, PMID 29253968.

46. Grip J, Engstad RE, Skjæveland I, Skalko Basnet N, Isaksson J, Basnet P. Beta-glucan-loaded nanofiber dressing improves wound healing in diabetic mice. Eur J Pharm Sci. 2018;121:269-80. doi: 10.1016/j.ejps.2018.05.031, PMID 29864585.

47. Silva JA, De Gregorio PR, Rivero G, Abraham GA, Nader Macias ME. Immobilization of vaginal lactobacillus in polymeric nanofibers for its incorporation in vaginal probiotic products. Eur J Pharm Sci. 2021;156:105563. doi: 10.1016/j.ejps.2020.105563, PMID 32976956.

48. Nageeb El-Helaly S, Abd-Elrasheed E, Salim SA, Fahmy RH, Salah S, El-Ashmoony MM. Green nanotechnology in the formulation of a novel solid dispersed multilayered core-sheath raloxifene-loaded nanofibrous buccal film; *in vitro* and *in vivo* characterization. Pharmaceutics. 2021;13(4):1-25. doi: 10.3390/pharmaceutics13040474, PMID 33915828, PMCID PMC8066100.

49. Kalluri L, Satpathy M, Duan Y. Effect of electrospinning parameters on the fiber diameter and morphology of plga nanofibers. Dent Oral Biol Craniofacial Res. 2021;4(2):1-19. doi: 10.31487/j.dobcr.2021.02.04, PMID 36970249, PMCID PMC10035641.

50. Silva P, Prieto C, lagaron J, Pastrana l, Coimbra M, Vicente A. Food-grade hydroxypropyl methylcellulose-based formulations for electrohydrodynamic processing: Part I–role of solution parameters on fibre and particle production. Food Hydrocoll. 2021;118:1-9.

51. Tam N, Oguz S, Aydogdu A, Sumnu G, Sahin S. Influence of solution properties and pH on the fabrication of electrospun lentil flour/HPMC blend nanofibers. Food Res Int. 2017;102:616-24. doi: 10.1016/j.foodres.2017.09.049, PMID 29195993.

52. Alishahi M, Khorram M, Asgari Q, Davani F, Goudarzi F, Emami A. Glucantime-loaded electrospun core-shell nanofibers composed of poly(ethylene oxide)/gelatin-poly(vinyl alcohol)/chitosan as dressing for cutaneous leishmaniasis. Int J Biol Macromol. 2020;163:288-97. doi: 10.1016/j.ijbiomac.2020.06.240, PMID 32610052.

53. Yin J, Fang Y, Xu L, Ahmed A. High-throughput fabrication of silk fibroin/hydroxypropyl methylcellulose (SF/HPMC) nanofibrous scaffolds for skin tissue engineering. Int J Biol Macromol. 2021;183:1210-21. doi: 10.1016/j.ijbiomac.2021.05.026, PMID 33984383.

54. Fatimah Mohammed Hussein Wais. Solubility and dissolution rate enhancement of ketoprofen by nanoparticles. Indian J Forensic Med Toxicol. 2020;14(4):2410-7. doi: 10.37506/ijfmt.v14i4.11949.